d-wave checkerboard order in cuprates

K. J. Seo   H. D. Chen

J. P. Hu

d-wave checkerboard order in cuprates

Kangjun Seo,[1] Han-Dong Chen,[2] and Jiangping Hu[1]

[1]*Department of Physics, Purdue University, West Lafayette, Indiana 47907, USA*
[2]*Department of Physics, University of Illinois at Urbana-Champaign, Urbana, Illinois 61801, USA*
(Received 15 May 2007; published 26 July 2007)

We show that the *d*-wave ordering in particle-hole channels, dubbed *d*-wave checkerboard order, possesses important physics that can sufficiently explain the scanning tunneling microscopy (STM) results in cuprates. A weak *d*-wave checkerboard order can effectively suppress the coherence peak in the single-particle spectrum while leaving the spectrum along the nodal direction almost unaffected. Simultaneously, it generates a Fermi arc with little dispersion around the nodal points at finite temperature that is consistent with the results of angle-resolved photoemission spectroscopy (ARPES) experiments in the pseudogap phase. We also show that there is a general complementary connection between the *d*-wave checkerboard order and the pair-density-wave order. Suppressing superconductivity locally or globally through phase fluctuations should induce both orders in underdoped cuprates and explain the nodal-antinodal dichotomy observed in ARPES and STM experiments.

PACS number(s): 74.25.Jb, 74.25.Dw, 74.72.−h

Recently, scanning tunneling microscopy (STM) has revealed surprising yet important electronic structures in the high-temperature superconductors. The Fourier transform scanning tunneling spectroscopies (FT-STSs) from STM have captured two different general features in both momentum and energy spaces.[1–9] One feature is dispersive peaks in FT-STSs,[4,5] interpreted as interference patterns caused by elastic scattering of quasiparticles from impurities.[10] The other is nondispersive peaks, a checkerboard modulation observed in various different materials and circumstances. The checkerboard structure was first discovered locally in BSCCO near a vortex core.[1,11] Then, it was found to be a characteristic of large-gap regions where the STM spectrum resembles that in the pseudogap phase.[2,5,7] Later, STM studies of $Ca_{2-x}Na_xCuO_2Cl_2$ revealed the presence of a global long-range commensurate checkerboard order independent of doping.[3] Finally, in the pseudogap phase, a similar checkerboard pattern was also observed.[6]

The origin of the checkerboard pattern has become central to understanding the nature of electronic states in cuprates. Various different mechanisms have been considered to explain the observed nondispersive checkerboard modulation, including pair density modulation,[12–16] current density modulation,[17,18] spin modulation,[19] stripe charge modulation,[20,21] impurity scattering,[22] and so on. Among the proposed mechanisms, the pair density wave (PDW) has been shown to capture important characteristics of the checkerboard density modulation. The mechanism of the PDW is derived from a high pairing energy scale in cuprates. It suggests that unlike the superconductivity of normal BCS-type superconductors that can be destroyed by breaking Cooper pairs, the superconductivity in cuprates can be more easily weakened or destroyed by phase fluctuations than by pair breaking. Based on this argument, pair density localization[12] was first proposed to explain local checkerboard modulation in the presence of an impurity or a vortex core. Later, a global PDW was proposed to explain the checkerboard physics in the pseudogap state.[6,13] It has also been shown that the symmetry of the tunneling intensity can distinguish pair density modulation from conventional density modulation.[13] While the pair density modulation provides a good understanding of the experimental results, it does not establish a direct link between superconducting and pseudogap states, as is suggested by the presence of the nondispersive checkerboard density modulation in both states. Furthermore, the theory has not explained three important features present in the STM spectrum: (i) the density of state at low energy in the superconducting state does not change whether or not a checkerboard modulation takes place locally, (ii) the overall intensity of the modulation is rather small, and (iii) the small modulation has a large effect on the STM spectrum around the superconducting gap.

In this Rapid Communication, we show that an explanation based on *d*-wave checkerboard density (DWCB) order in particle-hole channels can overcome the above limitations of the PDW theory. The DWCB can be viewed as a natural extension of the *d*-density-wave (DDW) order proposed to explain pseudogap physics[23,24] and is only different from the latter in terms of order wave vectors. We show that the DWCB order must exist when the PDW order is present in the global *d*-wave superconducting state. Moreover, we demonstrate that the DWCB order, with $\mathbf{Q}=\{(\pi/2,0),(0,\pi/2)\}$ and $f(\mathbf{k})=\cos(k_x)-\cos(k_y)$, can explain the STM experimental results. We show that the DWCB order has little effect on the density of state at low energy in the superconducting phase, but has a strong effect on the STM spectrum around the superconducting gap at high energy. This result naturally explains the puzzling dichotomy between the nodal and antinodal regions observed in STM[7] and angle-resolved photoemission spectroscopy (APRES).[25] The DWCB order also preserves in the FT-STSs spectrum at the wave vector $\mathbf{Q}$ the same symmetry as that observed in the experiments. Moreover, the DWCB preserves the nodes in the single-particle spectrum and generates a Fermi arc with little dispersion around the nodal points at high temperature, which are consistent with the results from ARPES. The Fermi arc has been a signature of the pseudogap region and has been proposed to explain the checkerboard pattern observed in the pseudogap state.[26] Thus, the DWCB provides a physical origin of the Fermi arc. In this Rapid Communication we present a model describing this physics.

The connection between particle-particle (P-P) and particle-hole (P-H) channel orders. To illustrate the complementary connection, we make use of the DDW order, since the only difference between the DWCB and DDW orders is the order wave vectors. Let us consider a state with a DDW order, $\langle \sum_\sigma c_{\mathbf{k}\sigma}^\dagger c_{\mathbf{k}+\mathbf{Q}'\sigma}\rangle = i\Delta_{\mathrm{DDW}}f(\mathbf{k})$, and a d-wave superconducting (DSC) order, $\langle c_{\mathbf{k}\uparrow}c_{-\mathbf{k}\downarrow}\rangle = \Delta_{\mathrm{DSC}}f(\mathbf{k})$, where $\mathbf{Q}' = (\pi, \pi)$. Some simple calculations will show that in the above mixed state of DDW and DSC, there naturally exists a PDW order with a wave vector at $\mathbf{Q}'$, given by

$$\langle c_{\mathbf{k}\uparrow}c_{-\mathbf{k}+\mathbf{Q}'\downarrow}\rangle \propto i\Delta_{\mathrm{DDW}}\Delta_{\mathrm{DSC}}f^2(\mathbf{k}). \tag{1}$$

This indicates that the mixed state of DDW and DSC has a complementary description as a mixed state of PDW and DSC. It is important to note that the symmetry of the PDW order in this case is an extended s wave. It is also easy to see that the symmetries of the order in the P-P channel and that in the P-H channel must be correlated with each other: if one is the extended s wave, the other is the d wave and vice versa. The above result holds for the DWCB order by replacing $\mathbf{Q}'$ by $\mathbf{Q}$. In a global DSC state, DWCB order must exist when a checkerboard PDW order is present. The complementary connection suggests that if the phase fluctuation leads to a Cooper pair modulation pattern, the orders in both the P-P and P-H channels have to be simultaneously considered in microscopic models.

Bogoliubov–de Gennes (BdG) equation and coexistence of PDW and DWCB order. To verify the existence of the DWCB order and the above complementary connection, we perform a self-consistent BdG calculation. We start from the following general Hamiltonian on a two-dimensional square lattice with nearest-neighbor attractive density interaction,

$$H = -\frac{1}{2}\sum_{\langle ij\rangle}[t_{ij}c_i^\dagger c_j + \mathrm{H.c.}] + \sum_{\langle ij\rangle}V_{ij}n_i n_j - \mu\sum_i n_i. \tag{2}$$

The density interaction V_{ij} includes two parts,

$$V_{ij} = V^0 + \delta V_{\mathbf{r}_i,\mathbf{r}_j} \tag{3}$$

where V^0 favors a d-wave superconducting state and $\delta V_{\mathbf{r}_i,\mathbf{r}_j}$ describes a modulating density interaction which creates a small checkerboard modulation on the top of the uniform superconducting state,

$$\delta V_{\mathbf{r},\mathbf{r}'} = V'_{\mathbf{r}'-\mathbf{r}}(\cos(\mathbf{Q}\cdot\mathbf{r}) + \cos(\mathbf{Q}\cdot\mathbf{r}')), \tag{4}$$

where $V'_{\hat{x}} = V'$ and $V'_{\hat{y}} = -V'$. The difference in the signs of $V'_{\hat{x}}$ and $V'_{\hat{y}}$ provides us the d-wave symmetry in the P-H channel order. We also note that the sign difference does not break rotational symmetry with respect to a proper rotation center in the lattice.

Starting with Eq. (2), we can derive the BdG equations by introducing mean-field decoupling of the nearest-neighbor interaction terms and obtain a self-consistent solution. The Bogoliubov–de Gennes equation is given by

$$\begin{pmatrix} \hat{H}_0 & \hat{\Delta}^* \\ \hat{\Delta} & -\hat{H}_0^* \end{pmatrix}\begin{pmatrix} u_n(\mathbf{r}) \\ v_n(\mathbf{r}) \end{pmatrix} = E_n\begin{pmatrix} u_n(\mathbf{r}) \\ v_n(\mathbf{r}) \end{pmatrix}, \tag{5}$$

where $\hat{H}_0$ and $\hat{\Delta}$ are transfer matrices such that

$$\hat{H}_0\psi_n(\mathbf{r}) = -\left(\sum_\delta[t + W_\delta(\mathbf{r})] + \mu(\mathbf{r})\right)\psi_n(\mathbf{r}+\delta), \tag{6}$$

$$\hat{\Delta}\psi_n(\mathbf{r}) = \sum_\delta \Delta_\delta(\mathbf{r})\psi_n(\mathbf{r}+\delta), \tag{7}$$

where $\psi_n(\mathbf{r})$ can be either $u_n(\mathbf{r})$ or $v_n(\mathbf{r})$, and δ denotes nearest-neighbor vectors. The order parameters are self-consistently determined by the self-consistent equations: the d-wave pairing amplitude on a bond $(\mathbf{r},\mathbf{r}+\delta)$ is given by

$$\Delta_\delta^{(1)}(\mathbf{r}) = V^0\langle c_{\mathbf{r}\downarrow}c_{\mathbf{r}+\delta\uparrow} + c_{\mathbf{r}+\delta\downarrow}c_{\mathbf{r}\uparrow}\rangle/2, \tag{8}$$

the pair-density-wave order in the P-P channel is

$$\Delta_\delta^{(2)}(\mathbf{r}) = \delta V_{\mathbf{r},\mathbf{r}+\delta}\langle c_{\mathbf{r}\downarrow}c_{\mathbf{r}+\delta\uparrow} + c_{\mathbf{r}+\delta\downarrow}c_{\mathbf{r}\uparrow}\rangle/2, \tag{9}$$

and the density order in the P-H channel is

$$W_\delta(\mathbf{r}) = -\delta V_{\mathbf{r},\mathbf{r}+\delta}\langle c_{\mathbf{r}\sigma}^\dagger c_{\mathbf{r}+\delta\sigma}\rangle. \tag{10}$$

We have numerically solved the BdG equation with various different parameter settings including different band structures in the square lattice with different $N\times N$ sizes. We find that the coexistence of the PDW and DWCB orders and the symmetry correspondence between them are the robust results in our calculation for this system. For example, with a parameter setting $V^0 = 2.5t$ and $V' = t$, the results are given by, for $\mathbf{r}' - \mathbf{r} = \hat{x}$ or $\hat{y}$, $\Delta_{\mathbf{r}'-\mathbf{r}}^{(1)}(\mathbf{r}) = \pm\Delta_0$, $\Delta_{\mathbf{r}'-\mathbf{r}}^{(2)}(\mathbf{r}) = \Delta_1(\cos(\mathbf{Q}\cdot\mathbf{r}) + \cos(\mathbf{Q}\cdot\mathbf{r}'))$, and $W_{\mathbf{r}'-\mathbf{r}}(\mathbf{r}) = \pm W_0(\cos(\mathbf{Q}\cdot\mathbf{r}) + \cos(\mathbf{Q}\cdot\mathbf{r}'))$ with $\Delta_0 = 0.3t$, $\Delta_1 = 0.25t$, and $W_0 = 0.15t$, which correspond to a state with

$$\Delta_{\mathrm{DSC}}(\mathbf{r}) = \Delta_0, \tag{11}$$

$$\Delta_{\mathrm{PDW}}(\mathbf{r}) = \Delta_1\cos(\mathbf{Q}\cdot\mathbf{r}), \tag{12}$$

$$W_{\mathrm{DWCB}}(\mathbf{r}) = W_0\cos(\mathbf{Q}\cdot\mathbf{r}). \tag{13}$$

We note that the PDW and DWCB orders have the same spatial modulation as $\cos(\mathbf{Q}\cdot\mathbf{r})$, while the symmetries of the PDW and DWCB orders are extended s-wave and d-wave symmetries, respectively. As shown in Fig. 1, DWCB has $4a\times 4a$ periodicity and d-wave symmetry. Similar order parameters have been mentioned in Ref. 22. The solutions are independent of the initial guesses for the local variables and converge quickly as N increases.

After demonstrating the coexistence of the DWCB and PDW orders, now we are interested in the physical effects of the DWCB order. To obtain a clear picture of the DWCB order, we illustrated a static pattern of the bond strength of the DWCB order in Fig. 1:

$$W_{\hat{x}}(\mathbf{r}) = \mathrm{Re}(W_0)\left[\cos\frac{\pi x}{2} - \sin\frac{\pi x}{2} + \cos\frac{\pi y}{2}\right], \tag{14}$$
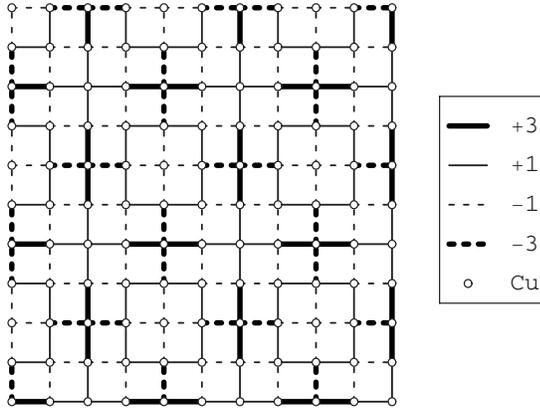
FIG. 1. The configuration of the bond density of DWCB order, or $W_\delta(r)$. It is manifestly shown that the pattern has $4a \times 4a$ periodicity and $d_{x^2-y^2}$ symmetry.

$$W_{\hat{y}}(\mathbf{r}) = -\operatorname{Re}(W_0)\left[\cos\frac{\pi y}{2} - \sin\frac{\pi y}{2} + \cos\frac{\pi x}{2}\right]. \quad (15)$$

It is clear that the DWCB order has $4a \times 4a$ periodicity and $d_{x^2-y^2}$ symmetry. Similar order parameters have been mentioned in Ref. 22.

Now we numerically calculate the average density of states (DOS), $\rho(\omega)$, and the Fourier components $\rho_\mathbf{Q}(\omega)$ at the wave vectors of the DWCB order, $\mathbf{Q}=\{(\pi/2,0),(0,\pi/2)\}$, and directly compare them with experimental results. We calculate the above quantities in two situations with different band dispersions. The results are rather general and are insensitive to the bare band structures. First, we performed calculations in the particle-hole-symmetric case. For a simple band dispersion, we choose $t=-125$ meV and $\mu=0$. $\Delta_0=40$ meV, which is relevant for underdoped BSCCO. The imaginary part of the self energy $\eta=5$ meV is used for the entire numerical calculation. Figure 2(a) shows the average DOS $(\mathbf{Q}=(0,0))$ normalized by the noninteracting Fermi liquids. In the absence of DWCB order, there are sharp coherence peaks at the energy of superconducting gap. As DWCB order develops, the coherence peaks are suppressed and pushed away while the spectrum at low energy remains unchanged. Figure 2(b) shows the Fourier components of the local density of states (LDOS) at the wave vectors $\mathbf{Q}$. As expected, $\rho_\mathbf{Q}(\omega)$ is even with respect to ω—namely, $\rho_\mathbf{Q}(\omega) = \rho_\mathbf{Q}(-\omega)$. Second, we repeat our calculations with the band dispersion provided by Norman *et al.*[27] and the result is displayed at the inset in Fig. 2(a). The band energy dispersion is now modified such that

$$\begin{aligned}\xi_\mathbf{k} = &\, t_1/2(\cos k_x + \cos k_y) + t_2 \cos k_x \cos k_y \\ &+ t_3/2(\cos 2k_x + \cos 2k_y) \\ &+ t_4/2(\cos 2k_x \cos k_y + \cos k_x \cos 2k_y) \\ &+ t_5 \cos 2k_x \cos 2k_y - \mu,\end{aligned} \quad (16)$$

where $t_1=-0.5951$ eV, $t_2=0.1636$ eV, $t_3=-0.0519$ eV, $t_4=-01117$ eV, and $t_5=0.0510$ eV. The chemical potential μ is now set to -0.1660 eV. Compared with the particle-hole-symmetric case, the effect of DWCB order on the LDOS is
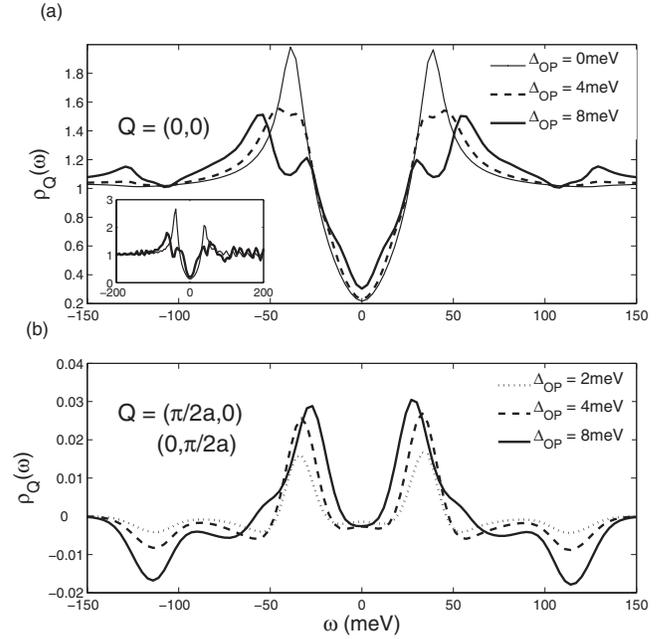

FIG. 2. (a) The average DOS in the particle-hole-symmetric case. The inset shows the average DOS with the finite chemical potential included in the band dispersion provided by Norman *et al.* (Ref. 27). Δ_{OP} represents W_0. (b) The Fourier components of the LDOS at $\mathbf{Q}=\{(\pi/2,0),(0,\pi/2)\}$.

insensitive to the energy band structure. Qualitatively the numerical results are strikingly consistent with experimental results[2,9] and the large gap region can be represented by the presence of DWCB order which is weak at $8-12$ meV.

Analytically, the general features in STM measurements can be captured by the DWCB order. First, due to the anisotropy inherited from the d-wave factor of pairing, a weak DWCB order has a much stronger effect on the antinodal region than on the nodal region, thus naturally explaining the puzzling dichotomy between the nodal and antinodal excitations in high-temperature superconductors: The local phase fluctuations of Cooper pairs lead to a local modulation of d-wave ordering in the particle-hole channel, which strongly affects the antinodal single-particle excitations. Second, like PDW order, DWCB order is bond centered and, consequently, $\rho_\mathbf{Q}(\omega)$ is an even function of ω, too.[13] The symmetry has been shown to distinguish the PDW from the typical particle-hole charge density wave (CDW). The existing experimental results are consistent with the even case.

The above result demonstrates the consistency between the DWCB order and the STM experimental results in the superconducting state. Now we show that the DWCB order also captures important physics in the pseudogap phase. One important feature of the pseudogap phase is the nondispersive Fermi arc developed from the nodal point along the Fermi surface observed in ARPES.[6] The Fermi arc has been used to explain the STM result in the pseudogap phase.[26] If the pseudogap phase is strongly connected to the phase fluctuations of d-wave superconductivity, the single-particle spectrum should reflect the DWCB order. Therefore, a robust Fermi arc feature should exist in the mixed DWCB and DSC phases at high temperature. We found that this is indeed the case.
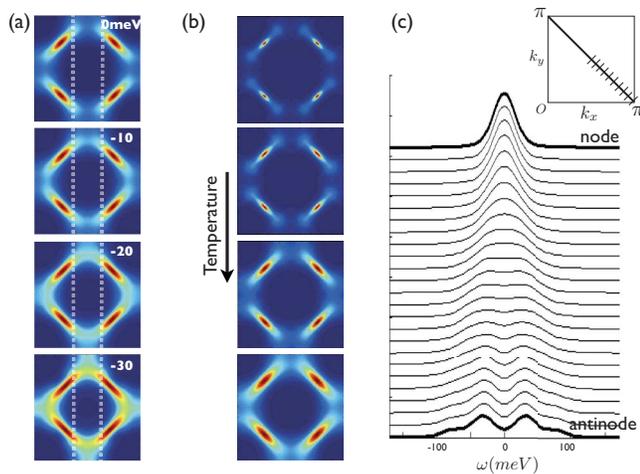
FIG. 3. (Color online) (a) With DSC and DWCB orders coexisting, the spectral weights $A(\mathbf{k}, \omega)$ are plotted as a function of ω (-30–0 meV) in the first Brillouin zone (BZ). Here we used $t=-125$ meV, $t'=\mu=0$ meV, and $T=120$ K. Each BZ is segmented by 100×100. White dotted lines indicate the nondispersive Fermi arcs. (b) Temperature dependence of $A(\mathbf{k}, \omega)$ at the Fermi level, $\omega=0$ meV. (c) Energy distribution curves from the nodal to antinodal point along the Fermi surface show the gapless region, or Fermi arc.

In Fig. 3, we have calculated $A(\mathbf{k}, \omega)$ in the pseudogap state within the model of Franz and Millis.[28] Figure 3(a) shows the numerical solutions of the spectral weight, $A(\mathbf{k}, \omega)$, as a function of ω at high temperature $T=120$ K where $\Delta_0=40$ meV and the DWCB order is equal to 8 meV. As expected in the pseudogap state, the scattering vector connecting the tips of Fermi arcs unchanges as the energy ω increases and is nearly equal to wave vectors of the d-checkerboard-order parameter, $|\mathbf{Q}|=\pi/2$. Figure 3(c) shows the spectral weight at $\omega=0$ for the cuts perpendicular to the Fermi arc which matches the experimental results.[26] For the temperature dependence, the length of the Fermi arc is linearly increasing as the temperature rises above T_c.[29] As seen in Fig. 3(c), at very low temperature the Fermi surface is gapped except for the nodal point $(\pi/2, \pi/2)$. As the temperature rises, the gapless region is elongated along the Fermi surface, with a slight broadening in the direction perpendicular to the Fermi surface.

In summary, DWCB order offers a unified explanation for the STM experiments in both the superconducting and pseudogap phases. A number of important issues need to be addressed. First, while we show that a complementary connection exists between the d-wave order in the particle-hole channel and the pair-density-wave order in the particle-particle channel, the order wave vectors should be determined by microscopic models. In general, pair fluctuations in different mircoscopic models can lead to different order wave vectors in the particle-hole channel. For example, the pair fluctuation can be anisotropic in the space that breaks the rotational lattice symmetry and will result in a stripelike one-dimensional ordering. Second, it is interesting that in a recent renormalization group study of the electron phonon interaction in cuprates, the authors have shown that DWCB order rises from coupling to half breathing or B_{1g} phonons.[30] Combining their results with ours suggests that the superconducting phase fluctuations may be strongly coupled with phonons. This hypothesis is of great importance and in need of future investigation. Finally, although a full calculation based on the BdG equation with DWCB order is yet to be completed, preliminary results show that the qualitative conclusion drawn here should remain valid.

In conclusion, the order in particle-hole channels—i.e., the DWCB order—can explain the STM spectrum and the nodal-antinodal dichotomy observed in both STM and ARPES experiments.[7,25] The presence of DWCB order also preserves the gapless dispersion at nodal points and simultaneously generates a Fermi arc with little dispersion around nodal points at finite temperature. The results are consistent with ARPES experiments and provide an explicit physical explanation of the Fermi arc in the pseudogap phase.

[1] J. E. Hoffman *et al.*, Science **295**, 466 (2002).
[2] C. Howald *et al.*, Phys. Rev. B **67**, 014533 (2003).
[3] T. Hanaguri *et al.*, Nature (London) **430**, 1001 (2004).
[4] K. McElroy *et al.*, Nature (London) **422**, 592 (2003).
[5] K. McElroy *et al.*, Physica C **388**, 225 (2003).
[6] M. Vershinin *et al.*, Science **303**, 1995 (2004).
[7] K. McElroy *et al.*, Phys. Rev. Lett. **94**, 197005 (2005).
[8] K. McElroy *et al.*, Science **309**, 1048 (2005).
[9] A. C. Fang *et al.*, Phys. Rev. Lett. **96**, 017007 (2006).
[10] Q.-H. Wang and D.-H. Lee, Phys. Rev. B **67**, 020511(R) (2003).
[11] S. H. Pan *et al.*, Phys. Rev. Lett. **85**, 1536 (2000).
[12] H. D. Chen *et al.*, Phys. Rev. Lett. **89**, 137004 (2002).
[13] H. D. Chen *et al.*, Phys. Rev. Lett. **93**, 187002 (2004).
[14] H.-D. Chen *et al.*, Phys. Rev. B **70**, 024516 (2004).
[15] Z. Tesanovic, Phys. Rev. Lett. **93**, 217004 (2004).

[16] A. Melikyan and Z. Tesanovic, Phys. Rev. B **71**, 214511 (2005).
[17] C. Bena *et al.*, Phys. Rev. B **69**, 134517 (2004).
[18] A. Ghosal *et al.*, Phys. Rev. B **72**, 220502(R) (2005).
[19] S. Sachdev and E. Demler, Phys. Rev. B **69**, 144504 (2004).
[20] S. A. Kivelson *et al.*, Rev. Mod. Phys. **75**, 1201 (2003).
[21] J. A. Robertson *et al.*, Phys. Rev. B **74**, 134507 (2006).
[22] D. Podolsky *et al.*, Phys. Rev. B **67**, 094514 (2003).
[23] C. Nayak, Phys. Rev. B **62**, 4880 (2000).
[24] S. Chakravarty *et al.*, Phys. Rev. B **63**, 094503 (2001).
[25] X. J. Zhou *et al.*, Phys. Rev. Lett. **92**, 187001 (2004).
[26] U. Chatterjee *et al.*, Phys. Rev. Lett. **96**, 107006 (2006).
[27] M. R. Norman *et al.*, Phys. Rev. B **52**, 615 (1995).
[28] M. Franz and A. J. Millis, Phys. Rev. B **58**, 14572 (1998).
[29] A. Kanigel *et al.*, Nat. Phys. **2**, 447 (2006).
[30] H. C. Fu *et al.*, arXiv:cond-mat/0509072 (unpublished).